PERGAMON

International Journal of Solids and Structures 38 (2001) 2713–2736

INTERNATIONAL JOURNAL OF SOLIDS and STRUCTURES

www.elsevier.com/locate/ijsolstr

Vibration analysis of laminated cylindrical thin panels with twist and curvature

Xiaxia Hu [a,*], Tsuneo Tsuiji [b]

[a] College of Mechanical and Electrical Engineering, Zhejiang University of Technology, Hangzhou 310014, Zhejiang, People's Republic of China

[b] Formerly at Department of Structural Engineering, Faculty of Engineering, Nagasaki University, 1-14 Bunkyomachi, Nagasaki 852, Japan

Received 12 March 1998; in revised form 10 April 2000

Abstract

Using the principle of virtual work and the Rayleigh–Ritz method with two dimensional algebraic polynomial displacement functions, the governing equation of vibration for a laminated cylindrical thin panel with twist and curvature is presented. The practicability and effectiveness of the method is verified by comparing the numerical results with those obtained by other researchers using experimental and other numerical methods. The effects of twist, curvature, characteristics of material, the number of layers, stacking sequence and fiber orientation on vibration frequency parameters of a laminated cylindrical thin panel with twist and curvature are studied, and some vibration mode shapes are also plotted to explain the variations of the vibration caused by them. © 2001 Elsevier Science Ltd. All rights reserved.

Keywords: Cylindrical panels; Rayleigh–Ritz method; Vibration frequency; Vibration mode shapes

1. Introduction

Manifold applications of shells have called attention to the study of their static and dynamic characteristics. There are a lot of researchers to devote themselves to this area. The recent studies on the vibrations of shallow shells are summarized in great detail (Liew et al., 1997). A cantilevered shell, which is an important structural component used in turbomachinery, impeller and fan blades, is a typical shell. There are hundreds of studies in the literature about the vibration analysis of turbomachinery blades (Leissa, 1981a,b). However, the turbomachinery blades were simplified as a cantilevered beam in the vast majority, and the representation was merely suitable to the blades with a large aspect ratio. The more accurate models were proposed by Leissa, Tsuiji, Liew and other researchers. Two-dimensional plates, shallow shells, cylindrical thin panels and shallow conical shells are used as models of turbomachinery blades (Leissa et al., 1982, 1983; Leissa, 1973; Tsuiji and Sueoka, 1990; Liew et al., 1994, 1995). To verify the practicability and accuracy of them, a large number of models were studied by the several numerical

* Corresponding author.

PII: S0020-7683(00)00178-5

methods, and experimental investigations were also carried out. Meanwhile, in-depth studies have been made on the effects of thickness, twist and curvature in the spanwise and the chordwise directions on the vibration characteristics.

With the development of composite materials and applications, it is known that the superior mechanical properties such as high strength and light weight can be obtained by selecting fiber orientation, stacking sequence, the number of layers in order to meet different applications in various engineering. Recently, the studies on the vibrations of blades treated as laminated shallow shell, laminated plate with twist and curvature and laminated shallow conical shell models were carried out by Qatu and Leissa (1991a,b), Tsuiji et al. (1996), Lim and Liew (1995), Lim et al. (1997, 1998) and Liew and Lim (1996), and the effects of various parameters such as twist, curvature, material, fiber orientation and the number of layers on the vibrations were also studied.

In this paper, a precise model of laminated turbomachinery blades, which is a laminated twisted and curved cylindrical thin panel, is proposed. The governing eigenvalue equation is derived by using the principle of virtual work for free vibration and the Rayleigh–Ritz method. For a model, the first 10 frequency parameters are presented and some vibration mode shapes are also plotted, and the effects of twist, curvature, characteristics of material, fiber orientation, the number of layers and stacking sequence on them are studied.

2. Mathematical formulation

A laminated cylindrical thin panel with twist and curvature is illustrated in Fig. 1, where a coordinate system xyz' with the origin O and a cylindrical coordinate system with the origin O_1 at the center of the cylinder are introduced. x is a curvilinear axis in the lengthwise direction and the twisting center axis, z'-axis takes in the radial direction where the cylindrical arc is equally divided into two parts, y-axis is chosen in such a way that the x-, y- and z'-axes form a right hand system, O is a point on the z'-axis, $\boldsymbol{i}_1$, $\boldsymbol{i}_2$ and $\boldsymbol{i}_3$ are the unit vectors of the coordinate system xyz', θ is the angle measured from the z'-axis, s-axis takes in the circumferential direction on the middle surface. Ω_1, r and b are the central angle, the average radius and the length of the cylindrical arc, respectively. t is the thickness of the panel ($t = \sum_i^M t_i$, M is the number of layers and t_i is the thickness of ith lamina). $1/R$ is the curvature of the x-axis, l is the length of the panel along the

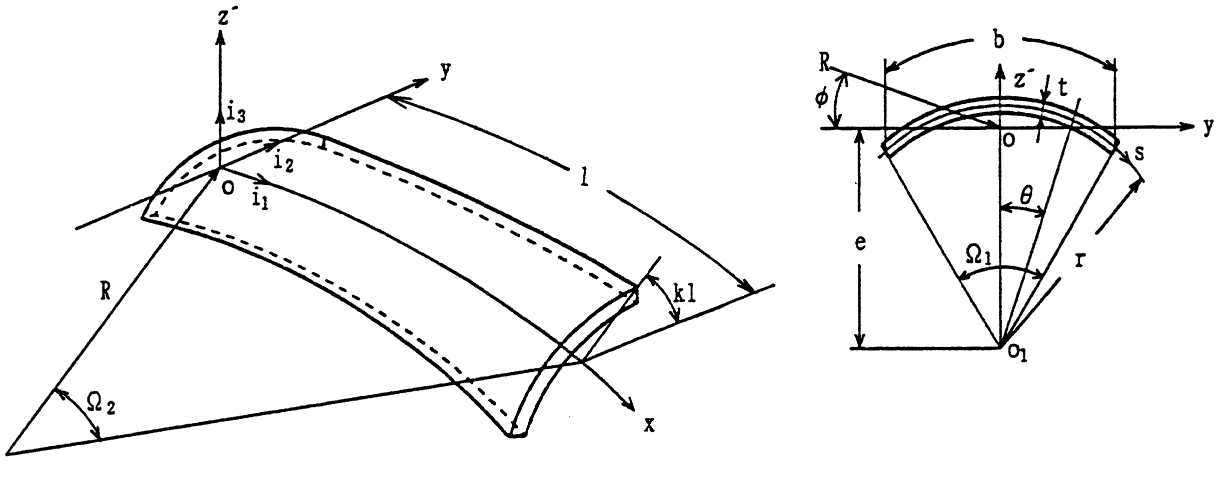

Fig. 1. A laminated cylindrical thin panel with twist and curvature.

x-axis, Ω_2 (l/R) is the central angle, k is the twisting angle per unit length, e is the distance between the points O and O_1. ϕ is an angle between the y-axis and the radial direction of the x-axis at the fixed end of the panel, and kl is the twisting angle at the free end of the panel.

It is assumed that the panel is laminated from an arbitrary number of perfectly bonded, elastic, anisotropic laminae having uniform thicknesses. For each lamina, the fiber orientation angle α lies between the fibers and the x-axis upon the projection of the x–y plane.

For the panel, displacement components U, V and W of an arbitrary point in the directions of the base vectors are expressed by displacement components u, v and w of a point which is a projected point of an arbitrary point on the middle surface of the panel in the radial direction (Hu and Tsuiji, 1999),

$$\begin{aligned} U &= \left(1 + z\frac{1}{B}h_4\right)u - z\frac{ek}{B^3 r}h_3 v - z\frac{1}{B^2}\frac{\partial w}{\partial x} + z\frac{k}{B^2 r}(e\cos\theta - r)\frac{\partial w}{\partial \theta}, \\ V &= -z\frac{k}{B}\left[1 + \frac{ek^2}{B^2 R}p\sin\theta(e\cos\theta - r)\right]u + \left\{1 + z\frac{1}{Br}\left[A + \frac{ek^2}{B^2}h_3(e\cos\theta - r)\right]\right\}v \\ &\quad + z\frac{k}{B^2}(e\cos\theta - r)\frac{\partial w}{\partial x} - z\frac{1}{r}\left[1 + \frac{k^2}{B^2}(e\cos\theta - r)^2\right]\frac{\partial w}{\partial \theta}, \\ W &= w, \end{aligned} \tag{1}$$

where z is the distance measured from the point to the middle surface, and the variables in the above equations and the following are defined in the Appendices A and B.

The strain–displacement relations are written as

$$\begin{bmatrix} \varepsilon_{xx} \\ \varepsilon_{\theta\theta} \\ \gamma_{x\theta} \end{bmatrix} = \frac{1}{F}\boldsymbol{ZGU}, \tag{2}$$

where matrices $\boldsymbol{Z}$, $\boldsymbol{G}$ and $\boldsymbol{U}$ are expressed by

$$\boldsymbol{Z} = \begin{bmatrix} 1 & \frac{z}{l} & \frac{z^2}{l^2} & 0 & 0 & 0 & 0 & 0 & 0 \\ 0 & 0 & 0 & 1 & \frac{z}{l} & \frac{z^2}{l^2} & 0 & 0 & 0 \\ 0 & 0 & 0 & 0 & 0 & 0 & 1 & \frac{z}{l} & \frac{z^2}{l^2} \end{bmatrix},$$

$$\boldsymbol{G} = \left[G_{i,j}\right] \quad (i = 1,9;\ j = 1,12),$$

$$\boldsymbol{U}^{\mathrm{T}} = \begin{bmatrix} \frac{\partial u}{\partial x} & \frac{\partial u}{\partial \theta} & u & \frac{\partial v}{\partial x} & \frac{\partial v}{\partial \theta} & v & \frac{\partial^2 w}{\partial x^2} & \frac{\partial^2 w}{\partial \theta^2} & \frac{\partial^2 w}{\partial x \partial \theta} & \frac{\partial w}{\partial x} & \frac{\partial w}{\partial \theta} & w \end{bmatrix}, \tag{3}$$

and the nonzero elements of matrix $\boldsymbol{G}$ are given in Appendix B.

The stress–strain relations for laminated composites are given by

$$\begin{bmatrix} \sigma_{xx} \\ \sigma_{\theta\theta} \\ \tau_{x\theta} \end{bmatrix} = \begin{bmatrix} \bar{Q}_{11} & \bar{Q}_{12} & \bar{Q}_{16} \\ \bar{Q}_{12} & \bar{Q}_{22} & \bar{Q}_{26} \\ \bar{Q}_{16} & \bar{Q}_{26} & \bar{Q}_{66} \end{bmatrix} \begin{bmatrix} \varepsilon_{xx} \\ \varepsilon_{\theta\theta} \\ \gamma_{x\theta} \end{bmatrix} = \bar{\boldsymbol{Q}} \begin{bmatrix} \varepsilon_{xx} \\ \varepsilon_{\theta\theta} \\ \gamma_{x\theta} \end{bmatrix}, \tag{4}$$

where $\bar{Q}_{ij}$ $(i,j = 1,2,6)$ are the transformed reduced stiffness coefficients, $\sigma_{xx}, \sigma_{\theta\theta}, \tau_{x\theta}$ and $\varepsilon_{xx}, \varepsilon_{\theta\theta}, \gamma_{x\theta}$ are stress and strain components, respectively.

The principle of virtual work for the free vibration of a twisted and curved cylindrical thin panel can be written as (Hu and Tsuiji, 1999)

$$\int\int\int_m \delta[\, \varepsilon_{xx} \quad \varepsilon_{\theta\theta} \quad \gamma_{x\theta}\,] \begin{bmatrix} \sigma_{xx} \\ \sigma_{\theta\theta} \\ \tau_{x\theta} \end{bmatrix} F\,\mathrm{d}x\,r\,\mathrm{d}\theta\,\mathrm{d}z - \int\int\int_m \rho\omega^2 \Big\{ \Big[B^2 + k^2 (r - e\cos\theta)^2 \Big] u\,\delta u$$
$$+ k(e\cos\theta - r)(v\,\delta u + u\,\delta v) + v\,\delta v + w\,\delta w \Big\} F\,\mathrm{d}x\,r\,\mathrm{d}\theta\,\mathrm{d}z = 0, \tag{5}$$

where ρ is the density of a material and ω is the angular frequency.

In order to present a generalized equation which is independent of a model's dimensions, the following dimensionless parameters are introduced:

$$\bar{x} = \frac{x}{l}, \quad \bar{u} = \frac{u}{l}, \quad \bar{v} = \frac{v}{l}, \quad \bar{w} = \frac{w}{l}, \quad \bar{r} = \frac{r}{l}, \quad \bar{e} = \frac{e}{r}, \quad \bar{k} = kl, \tag{6}$$

and substituting Eqs. (2), (4) and (6) into Eq. (5), then integrating with respect to z and neglecting terms which contain z^3 and higher, the dimensionless principle of virtual work for the free vibration of a laminated cylindrical thin panel with twist and curvature can be written as

$$\int\int_S \delta\bar{\boldsymbol{U}}^{\mathrm{T}} \bar{\boldsymbol{G}}^{\mathrm{T}} \bar{\boldsymbol{D}} \bar{\boldsymbol{G}} \bar{\boldsymbol{U}} \bar{r}\,\mathrm{d}\bar{x}\,\mathrm{d}\theta - \lambda^2 \int\int_S \Big\{ \Big[\bar{B}^2 + \bar{k}^2 \bar{r}^2 (1 - \bar{e}\cos\theta)^2 \Big] \bar{u}\,\delta\bar{u} + \bar{k}\bar{r}(\bar{e}\cos\theta - 1)(\bar{v}\,\delta\bar{u} + \bar{u}\,\delta\bar{v})$$
$$+ \bar{v}\,\delta\bar{v} + \bar{w}\,\delta\bar{w} \Big\} \bar{B}\bar{r}\,\mathrm{d}\bar{x}\,\mathrm{d}\theta = 0. \tag{7}$$

λ is the dimensionless frequency parameter defined as

$$\lambda^2 = \frac{\rho\omega^2 l^4}{E_1 t^2}, \tag{8}$$

where E_1 is Young's modulus of a composite material, and matrix $\bar{\boldsymbol{D}}$ is expressed as

$$\bar{\boldsymbol{D}} = \frac{l^2}{E_1 t^3} \int_{-t/2}^{t/2} \frac{1}{F} \boldsymbol{Z}^{\mathrm{T}} \bar{\boldsymbol{Q}} \boldsymbol{Z}\,\mathrm{d}z. \tag{9}$$

In the Rayleigh–Ritz method, the dimensionless displacements $\bar{u}, \bar{v}$ and $\bar{w}$ are assumed as two-dimensional algebraic polynomial functions of $\bar{x}$ and θ which satisfy the boundary conditions at $\bar{x} = 0$, namely, $\bar{u} = 0, \bar{v} = 0, \bar{w} = 0$ and $\partial\bar{w}/\partial\bar{x} = 0$. They can be written as

$$\bar{u} = \sum_{i=1}^{N_{\bar{u}}} \sum_{j=0}^{M_{\bar{u}}} a_{ij} \bar{x}^i \theta^j, \qquad \bar{v} = \sum_{k=1}^{N_{\bar{v}}} \sum_{l=0}^{M_{\bar{v}}} b_{kl} \bar{x}^k \theta^l, \qquad \bar{w} = \sum_{m=2}^{N_{\bar{w}}} \sum_{n=0}^{M_{\bar{w}}} c_{mn} \bar{x}^m \theta^n, \tag{10}$$

where a_{ij}, b_{kl} and c_{mn} are unknown coefficients.

By substituting Eq. (10) into Eq. (7), and integrating it over the area of a panel by the Gauss–Legendre numerical integration, the governing eigenvalue equation is presented in a matrix form as

$$(\boldsymbol{A} - \lambda^2 \boldsymbol{B})\boldsymbol{q} = 0, \tag{11}$$

where $\boldsymbol{A}$ and $\boldsymbol{B}$ are the stiffness and mass matrices, respectively, and $\boldsymbol{q}$ is the vector consisting of unknown coefficients a_{ij}, b_{kl} and c_{mn}.

By the aid of the Householder–QR method, the vibration frequency parameters and corresponding mode shapes for the free vibration of the panel can be evaluated from Eq. (11).

Table 1
Characteristic parameters of the two materials

Material	E_1 (GPa)	E_2 (GPa)	G_{12} (GPa)	v_{12}	E_1/E_2	G_{12}/E_2
E-glass/epoxy (E/E)	60.7	24.8	12.0	0.23	2.4476	0.4839
Graphite/epoxy (G/E)	138.0	8.96	7.1	0.30	15.402	0.7924

3. Analysis

The cylindrical thin panels consisting of two kinds of laminated composite materials are studied, respectively. The characteristic parameters of the materials are shown in Table 1.

3.1. Convergence property of solutions

In the present method, the two-dimensional algebraic polynomial functions are used as displacement functions and the Gauss–Legendre integration method is also used. Therefore, it is necessary to know the convergence property of the numerical solutions about the number of terms in the algebraic polynomials. The property is studied for a twisted and curved cylindrical thin panel composed of four-layer graphite/epoxy laminated composite with a stacking sequence $[60°/-60°]_s$. The geometric parameters of the panel are $\Omega_1 = 60°$, $\Omega_2 = 60°$, $\bar{k} = 60°$, $\phi = -90°$, an aspect ratio $l/b = 1$ and a thickness ratio $b/t = 20$.

The convergence of frequency parameters λ against the number of terms included in the displacement polynomials $\bar{u}$, $\bar{v}$ and $\bar{w}$ is shown in Table 2. Obviously, the frequency parameters λ converge when 12 integrating points are taken and the displacement functions $\bar{u}$, $\bar{v}$ and $\bar{w}$ having the maximum power terms of $\bar{x}^7\theta^7$, $\bar{x}^7\theta^7$ and $\bar{x}^8\theta^8$, respectively, are considered.

3.2. Comparison to previous solutions

First, the cantilevered cylindrical thin panels (Qatu and Leissa, 1991a) consisting of the laminated composite material with the following parameters $E_1 = 128$ GPa, $E_2 = 11$ GPa, $G_{12} = 4.48$ GPa, $v = 0.25$, $\rho = 1500$ kg/m^3, the thickness of a ply is 0.13 mm, $r = 12.75$ cm, $l = 15.24$ cm, the projection of b on the horizontal plane $b' = 7.62$ cm and twisting angle $\bar{k} = 0°$ for different stacking sequences are studied. The first five natural frequencies (Hz) of each model are calculated by the present method, and the comparisons

Table 2
Convergence of λ versus the maximum power of $(\bar{x}, \theta)$ in $\bar{u}, \bar{v}, \bar{w}$

No.	$\bar{u},\bar{v},\bar{w}$		
	(6, 7), (6, 7), (7, 8)	(7, 6), (7, 6), (8, 7)	(7, 7), (7, 7), (7, 8)
1	0.5060	0.5093	0.5050
2	1.7383	1.7372	1.7345
3	3.0254	3.0209	3.0183
4	4.1840	4.1571	4.1546
5	5.3692	5.3541	5.3475
6	6.1732	6.1091	6.1024
7	7.5421	7.4646	7.4564
8	8.9854	8.9202	8.9103
9	9.8657	9.2073	9.2022
10	11.9735	11.8632	11.8553

Table 3
Comparison of natural frequencies (Hz) for cylindrical panels

Method No.	Crawley		Present	Qatu and Leissa (1991a)
	FEM	Exp.		
Panel A: Laminates $[0°/0°/30°/-30°]_s$.				
1	165.7	161.0	168.3	163.8
2	289.6	254.1	293.0	269.5
3	597.0	555.6	593.9	593.0
4	718.5	670.0	726.2	702.5
5	833.3	794.0	834.2	824.8
Panel B: Laminates $[0°/45°/-45°/90°]_s$.				
1	192.4	177.0	194.2	190.8
2	236.1	201.8	240.0	217.5
3	705.8	645.0	711.6	695.5
4	808.2	754.0	803.8	804.8
5	980.6	884.0	984.5	958.1
Panel C: Laminates $[45°/-45°/-45°/45°]_s$.				
1	147.0	145.3	147.9	133.1
2	238.0	222.0	239.1	236.2
3	768.1	712.0	771.3	746.6
4	812.1	774.2	807.0	758.8
5	–	–	–	842.1
6	1038	997.0	1039	1037

with analytical and experimental data provided by Qatu and Leissa (1991a) are shown in Table 3. It can be seen that the experimental data are the smallest, and the data obtained by the present method are the greatest. The data obtained by the present method agree with Crawley's (FEM) results very well and the maximum difference is less than 2%. The discrepancy with those in Qatu and Leissa (1991a) is slightly larger and the maximum is 10.0%. It is worthy to note that the fifth mode in Table 3 (Panel C) obtained by Qatu and Leissa (1991a) did not appear when the other methods were used.

Second, for the three-layer $[45°/-45°/45°]$ laminated panels Qatu and Leissa (1991a) having the parameters $a'/b' = 1$, where a' is the projection of l on the horizontal plane, $b'/t = 100$ and $\phi = -90°$, the first 10 frequency parameters λ are obtained by the present method for different ratios of $r/R = \pm 1$ and $b'/r = 0.1, 0.5$ and compared with those shown in Qatu and Leissa (1991a). The results are shown in Table 4 for E-glass/epoxy laminated cylindrical panels and in Table 5 for graphite/epoxy ones. It can be seen that results obtained by the two different methods agree well. The maximum difference is less than 0.5% in the cases of $r/R = \pm 1$ and $b'/r = 0.1$, and 6.16% in the cases of $r/R = \pm 1$ and $b'/r = 0.5$. These mean that the maximum difference increases when the radii R and r increase. Because the method proposed by Qatu and Leissa (1991a) was based on the shallow shell theory, it is capable of representing the vibration characteristics accurately for shells having smaller curvatures and may be inadequate for shells having large curvatures. But the present method is based on the general shell theory, the precise results can be obtained by it even for shells having large curvatures and large twists.

3.3. Effects of parameters on vibration

For the panel with $l/b = 2$, $b/t = 100$ and $\phi = -90°$, the effects of parameters such as twist, curvature, characteristics of composite material, the number of layers, fiber orientation and stacking sequence on the

Table 4
Comparison of frequency parameters for E/E panels

b'/r	0.1				0.5			
r/R	+1		−1		+1		−1	
No.	Qatu and Leissa (1991a)	Present	Qatu and Leissa (1991a)	Present	Qatu and Leissa (1991a)	Present	Qatu and Leissa (1991a)	Present
1	1.0898	1.0915	1.0945	1.0959	2.0791	2.1138	1.7448	1.7882
2	2.1586	2.1627	2.1363	2.1407	2.4770	2.5898	2.4849	2.6010
3	5.1025	5.1077	5.7682	5.7706	7.1003	7.5076	7.5404	7.5566
4	7.0262	7.0393	7.0756	7.0797	8.2510	8.5916	9.6987	9.7530
5	8.0695	8.0844	8.0792	8.0843	11.877	12.541	16.366	16.622
6	14.034	14.061	12.920	12.931	16.813	17.637	19.907	20.347
7	14.453	14.464	14.552	14.556	20.602	21.688	23.215	24.045
8	15.085	15.114	15.501	15.521	22.738	24.155	25.692	27.071
9	17.648	17.680	17.221	17.233	32.507	34.010	28.047	29.445
10	21.607	21.586	20.841	20.844	33.375	35.157	32.316	33.717

Table 5
Comparison of frequency parameters for G/E panels

b'/r	0.1				0.5			
r/R	+1		−1		+1		−1	
No.	Qatu and Leissa (1991a)	Present	Qatu and Leissa (1991a)	Present	Qatu and Leissa (1991a)	Present	Qatu and Leissa (1991a)	Present
1	0.6845	0.6858	0.6448	0.6459	1.3063	1.3283	0.9234	0.9482
2	1.5593	1.5632	1.4700	1.4736	1.9174	2.0073	2.0704	2.1654
3	3.0442	3.0499	3.4879	3.4902	4.5013	4.7599	4.0276	4.0412
4	4.0921	4.1014	4.3262	4.3313	5.7639	6.0475	7.9421	7.9846
5	5.5496	5.5594	5.6651	5.6687	8.0385	8.5228	9.1653	9.3068
6	8.2623	8.2769	7.1957	7.2024	10.639	11.222	13.836	14.336
7	9.0504	9.0605	9.3124	9.3140	12.827	13.594	15.863	16.177
8	9.4966	9.5162	9.6236	9.6248	14.771	15.700	16.914	17.799
9	12.537	12.497	11.779	11.744	19.844	20.922	18.590	19.732
10	13.163	13.187	13.006	13.010	20.552	21.900	19.560	20.332

frequency parameters λ and mode shapes of laminated cylindrical thin panels are studied. The two materials, one having the moderately orthotropic E-glass/epoxy and another having the strongly orthotropic graphite/epoxy, are used. The first 10 vibration frequency parameters λ of the problems are presented and some mode shapes which are the contour plots of the displacement $\bar{w}$ are also plotted.

There are nine tables to show the changes in the frequency parameters caused by twist and fiber orientation for different panels, which are Tables 6–8 for three-layer graphite/epoxy laminated panels, Tables 9–11 for three-layer E-glass/epoxy and Tables 12–14 for four-layer graphite/epoxy ones. For a stacking sequence $[\alpha/-\alpha/\alpha]$, the maximum value of the first frequency parameter λ mostly occurs when the fibers are perpendicular to the clamped edges ($\alpha = 0°$), and for a stacking sequence $[\alpha/-\alpha/\alpha/-\alpha]$, it appears in the case of $\alpha = 0°$ when Ω_1 and Ω_2 are 30°, but the maximum point of λ moves to $\alpha = 15°$ when Ω_1 and Ω_2

Table 6
λ of G/E panels ($\Omega_1 = \Omega_2 = 30°$, $[\alpha/-\alpha/\alpha]$)

$\bar{k}$	α	1	2	3	4	5	6	7	8	9	10
0°	0°	1.912	2.194	8.101	9.221	13.83	19.83	24.81	28.86	40.30	41.65
	15°	1.737	2.700	8.475	9.392	15.05	19.87	25.25	30.76	38.82	42.13
	30°	1.550	3.187	8.046	9.752	16.30	19.49	25.18	31.44	37.22	42.69
	45°	1.398	3.099	7.113	9.584	15.36	19.06	23.52	30.30	34.99	42.41
	60°	1.308	2.544	6.447	8.423	14.24	17.61	22.13	27.49	31.24	38.73
	75°	1.307	1.940	5.650	7.533	12.33	16.55	21.08	24.91	28.54	33.35
	90°	1.391	1.602	5.172	7.214	11.17	16.11	19.32	24.32	28.78	29.87
15°	0°	1.701	2.532	8.216	9.046	14.09	20.22	24.24	29.42	39.93	41.44
	15°	1.415	2.792	7.261	9.038	14.24	18.10	23.71	30.06	35.59	40.67
	30°	1.302	2.935	6.829	8.831	14.91	16.68	23.38	29.01	33.90	40.14
	45°	1.315	2.611	6.822	7.991	14.46	16.16	21.88	27.94	32.16	39.71
	60°	1.276	2.244	6.443	7.286	13.48	15.71	21.12	25.48	29.36	37.67
	75°	1.078	2.166	5.336	7.400	11.62	16.13	19.98	24.26	27.41	33.73
	90°	0.912	2.394	4.889	7.517	11.31	15.95	19.58	24.65	28.57	30.51
30°	0°	1.440	3.276	7.918	9.750	15.12	21.23	23.81	30.53	38.97	41.08
	15°	1.113	3.180	6.463	8.798	14.36	16.94	22.76	30.66	32.35	39.58
	30°	0.937	3.223	5.379	8.741	13.89	14.94	22.48	27.04	31.43	38.50
	45°	0.897	3.078	5.269	8.441	13.58	14.45	21.83	24.91	30.91	37.57
	60°	0.814	2.918	5.226	7.970	12.71	15.14	20.93	23.49	29.02	36.91
	75°	0.686	2.785	4.998	7.488	11.95	15.41	19.93	24.29	27.65	34.69
	90°	0.629	2.814	5.141	7.434	12.54	15.14	21.01	25.48	29.10	31.51
45°	0°	1.256	4.347	7.211	12.90	16.51	23.59	25.68	31.27	39.06	41.42
	15°	0.944	3.766	6.312	10.76	15.21	19.97	24.27	31.35	33.48	39.38
	30°	0.699	3.342	5.380	9.333	14.03	17.50	24.29	28.10	33.41	38.42
	45°	0.608	2.968	5.502	8.370	14.05	15.91	23.83	25.41	34.17	36.79
	60°	0.557	2.657	5.906	7.482	14.50	15.17	23.00	23.95	31.84	36.49
	75°	0.496	2.395	6.116	6.769	13.47	15.35	22.40	24.89	30.25	34.81
	90°	0.487	2.379	6.372	6.911	13.77	15.58	23.37	26.51	31.15	32.85
60°	0°	1.157	4.855	7.772	15.55	19.96	27.72	30.16	32.93	40.35	44.49
	15°	0.896	3.956	7.400	12.58	20.03	24.58	30.37	35.46	38.39	42.40
	30°	0.635	2.978	7.198	9.417	19.21	20.29	30.18	35.63	37.34	44.26
	45°	0.492	2.328	7.137	7.889	17.30	18.11	29.06	31.57	37.42	41.66
	60°	0.439	2.035	6.357	8.011	15.28	18.68	26.21	28.47	35.62	40.90
	75°	0.403	1.863	5.814	8.045	13.52	18.81	25.67	26.62	33.95	37.26
	90°	0.409	1.888	5.843	8.409	13.27	18.82	25.56	27.92	34.27	35.18

become large. It can be seen that the first frequency parameter decreases monotonically with the increase of the twisting angle.

Generally, for a laminated panel with twist and curvature, the first frequency parameters mostly appears as the maximum in the case of $\alpha = 0°$ and appears as the minimum in the case of $\alpha = 90°$, and the difference between them becomes great when the twisting angle increases.This reduction is great when Ω_1 and Ω_2 are small, and it decreases with the increases in Ω_1 and Ω_2. For three-layer graphite/epoxy laminated panels, the maximum reduction occurs when the twisting angle $\bar{k}$ is 60°, which is 65% when Ω_1 and Ω_2 are 30°, 48% when Ω_1 and Ω_2 are 60°, and 36% when Ω_1 and Ω_2 are 90°. Those are 28%, 17% and 11% for three-layer E-glass/epoxy laminated panels having the same dimensions. The trend is the same as that Qatu and Leissa (1991a) mentioned. He pointed out that the change of the fiber orientation angle has much greater effect upon the fundamental frequency parameter for plates than for shells. It can also be seen that the changes in

Table 7
λ of G/E panels ($\Omega_1 = \Omega_2 = 60°$, $[\alpha/-\alpha/\alpha]$)

$\bar{k}$	α	1	2	3	4	5	6	7	8	9	10
0°	0°	2.196	2.218	7.962	10.27	15.69	21.21	31.47	31.81	45.77	50.84
	15°	1.985	2.750	8.644	10.32	17.16	21.80	32.40	34.24	47.41	53.14
	30°	1.832	3.160	9.296	9.943	19.08	21.85	32.83	35.94	49.85	52.48
	45°	1.728	3.065	8.383	10.19	18.58	21.65	30.60	35.69	47.38	50.89
	60°	1.671	2.661	7.203	10.06	17.35	21.09	27.43	33.47	41.27	50.23
	75°	1.637	2.229	6.152	9.717	15.60	20.84	26.54	29.42	36.42	45.56
	90°	1.620	2.034	5.649	9.499	14.52	20.51	26.59	27.20	34.26	42.61
15°	0°	2.077	2.345	7.930	10.20	15.44	21.28	29.99	32.55	45.47	50.63
	15°	1.819	2.738	8.201	9.921	16.17	20.92	30.02	33.96	44.95	51.64
	30°	1.722	2.958	8.768	9.223	17.62	20.42	30.45	34.17	46.67	50.29
	45°	1.757	2.680	8.094	9.290	17.18	20.30	28.22	34.14	44.58	48.75
	60°	1.888	2.168	7.003	9.400	16.33	20.11	25.60	32.65	39.11	48.62
	75°	1.688	2.067	6.013	9.413	14.98	20.31	25.32	29.30	35.15	44.99
	90°	1.410	2.336	5.638	9.469	14.44	20.45	26.13	27.61	34.23	42.46
30°	0°	1.916	2.567	8.002	9.939	14.87	21.48	27.91	32.70	44.52	50.09
	15°	1.622	2.804	7.672	9.475	14.91	20.09	27.07	33.39	42.09	49.35
	30°	1.564	2.874	8.047	8.713	15.98	19.06	27.41	32.81	42.52	47.92
	45°	1.662	2.557	7.863	8.444	15.78	19.04	25.69	32.86	40.81	46.83
	60°	1.636	2.333	6.810	8.829	15.20	19.24	23.93	31.73	36.60	47.29
	75°	1.336	2.502	5.884	9.125	14.18	19.83	24.13	29.06	33.86	44.49
	90°	1.148	2.833	5.656	9.327	14.31	20.18	25.49	28.20	34.23	42.22
45°	0°	1.715	2.976	8.625	9.407	14.58	21.93	25.86	32.51	43.18	49.06
	15°	1.396	3.024	7.405	8.949	14.03	19.30	24.52	32.73	39.20	46.88
	30°	1.321	3.033	7.186	8.527	14.75	17.76	24.79	31.88	38.04	45.89
	45°	1.370	2.849	7.343	8.173	14.86	17.78	23.80	31.86	36.76	45.31
	60°	1.260	2.834	6.655	8.495	14.26	18.52	22.82	30.57	34.34	46.44
	75°	1.044	2.983	5.925	8.789	13.60	19.36	23.13	28.80	33.00	44.42
	90°	0.938	3.211	5.949	8.953	14.45	19.53	25.18	28.82	34.59	42.22
60°	0°	1.499	3.611	8.647	10.37	15.23	22.89	24.71	32.80	42.04	47.25
	15°	1.172	3.410	7.382	9.123	14.54	18.76	23.91	33.03	37.27	45.23
	30°	1.047	3.409	6.447	9.036	14.85	16.78	24.29	31.79	35.67	45.13
	45°	1.056	3.323	6.662	8.756	14.92	16.83	23.69	30.72	35.21	44.61
	60°	0.966	3.241	6.730	8.471	14.02	18.14	22.82	29.32	33.81	46.43
	75°	0.827	3.135	6.551	8.250	13.78	18.56	23.13	28.74	33.36	45.09
	90°	0.779	3.147	6.917	8.315	15.06	18.52	25.61	29.43	35.71	42.59

higher frequency parameters are complicated, but they are smaller than those of lower frequency parameters.

For four-layer $[\alpha/-\alpha/\alpha/-\alpha]$ graphite/epoxy laminated panels, the changes in frequency parameters λ are shown in Tables 12–14. Comparing with three-layer ones, it can be seen that the variations caused by $\bar{k}$, Ω_1 and Ω_2 are almost the same and most of the frequency parameters λ are greater.

Figs. 2–10 are the mode shapes of the panels when Ω_1 and Ω_2 are 60°, and heavier lines are nodal lines which indicate that normal displacement $\bar{w}$ is zero. In each group of the modes, the first eight mode shapes are plotted for a graphite/epoxy or E-glass/epoxy laminated panel with a stacking sequence $[\alpha/-\alpha/\alpha]$ or $[\alpha/-\alpha/\alpha/-\alpha]$, a twisting angle $\bar{k} = 0°, 30°, 60°$ and a fiber orientation angle $\alpha = 0° - 90°$.

For three-layer $[\alpha/-\alpha/\alpha]$ graphite/epoxy laminated panels, the variations in the modes with the change of a fiber orientation angle are shown in Figs. 2–4. In the case of $\bar{k} = 0°$, when the fiber orientation angle α

Table 8
λ of G/E panels ($\Omega_1 = \Omega_2 = 90°$, $[\alpha/-\alpha/\alpha]$)

$\bar{k}$	α	1	2	3	4	5	6	7	8	9	10
0°	0°	2.199	2.613	8.520	10.88	17.22	23.87	34.06	37.44	53.12	58.78
	15°	2.263	2.847	9.290	11.05	18.87	24.62	36.81	39.00	55.80	63.19
	30°	2.195	3.103	10.26	10.66	21.17	24.63	39.18	40.30	59.30	63.22
	45°	2.070	3.018	9.284	11.12	20.86	24.33	36.53	40.93	57.26	59.64
	60°	1.922	2.784	7.936	11.28	20.06	23.40	32.13	39.81	50.67	58.30
	75°	1.736	2.593	6.854	11.01	18.75	23.34	29.65	35.84	44.86	56.25
	90°	1.633	2.518	6.355	10.76	17.79	23.33	28.97	33.38	41.98	53.79
15°	0°	2.184	2.616	8.373	10.93	16.89	23.82	33.33	37.12	52.94	58.59
	15°	2.128	2.853	9.001	10.77	18.03	24.04	34.66	38.59	53.70	61.79
	30°	2.104	2.977	9.912	10.08	19.81	23.67	36.52	38.97	56.43	61.34
	45°	2.108	2.743	8.803	10.68	19.38	23.36	34.16	39.47	54.27	58.23
	60°	2.055	2.461	7.609	10.92	18.81	22.81	30.30	38.82	48.64	57.15
	75°	1.768	2.468	6.667	10.81	18.03	23.07	28.47	35.56	43.66	55.22
	90°	1.582	2.601	6.341	10.72	17.70	23.30	28.88	33.33	41.95	53.25
30°	0°	2.129	2.664	8.122	10.97	16.06	23.61	31.62	36.21	51.57	58.60
	15°	1.960	2.892	8.424	10.66	16.70	23.26	31.75	37.43	51.14	59.75
	30°	1.989	2.913	9.188	9.951	18.10	22.69	33.11	37.59	52.45	58.96
	45°	2.122	2.572	8.407	10.31	17.78	22.53	31.17	38.22	50.45	56.63
	60°	2.070	2.352	7.357	10.55	17.47	22.44	28.10	37.88	45.89	56.30
	75°	1.666	2.567	6.512	10.56	17.10	22.96	27.08	35.12	42.22	54.10
	90°	1.460	2.824	6.330	10.58	17.45	23.21	28.62	33.16	41.89	52.11
45°	0°	2.002	2.871	8.149	10.92	15.26	23.26	29.79	35.15	49.13	58.96
	15°	1.756	3.024	7.928	10.47	15.35	22.42	28.77	35.99	47.99	57.97
	30°	1.804	3.002	8.583	9.801	16.47	21.77	29.62	36.39	47.86	56.43
	45°	1.925	2.737	8.222	9.912	16.48	21.82	28.16	37.22	46.09	54.94
	60°	1.791	2.674	7.301	10.16	16.30	22.19	25.91	36.97	42.55	55.60
	75°	1.484	2.858	6.492	10.26	16.15	22.82	25.73	34.47	40.60	53.06
	90°	1.312	3.130	6.411	10.31	17.11	22.94	28.27	32.89	41.78	50.91
60°	0°	1.807	3.302	8.726	10.79	15.24	23.06	28.46	34.74	46.98	59.07
	15°	1.533	3.299	7.936	10.23	14.84	21.83	26.82	35.39	45.75	56.06
	30°	1.558	3.300	8.328	9.636	15.70	21.08	27.20	36.09	44.71	54.62
	45°	1.635	3.161	8.365	9.526	15.89	21.22	25.97	36.73	42.34	53.95
	60°	1.515	3.137	7.545	9.819	15.51	21.93	24.30	36.15	39.46	55.09
	75°	1.291	3.240	6.744	9.916	15.41	22.46	24.72	33.77	39.11	52.24
	90°	1.165	3.413	6.752	9.924	16.78	22.42	27.88	32.69	41.57	49.89

changes from 0° to 30°, the first mode becomes the second one and the second mode becomes the first one, and they do not change when α changes from 30° to 60°, but they change back when α changes from 60° to 90°. The third mode also changes its order in the first eight modes when the fiber orientation changes, and it comes back to its original order when α changes from 60° to 90°. The sixth and seventh modes in the case of $\alpha = 0°$ become the fifth and sixth modes in the case of $\alpha = 90°$. From the modes of the panel with $\bar{k} = 0°$, it can be seen that two torsional modes appear when $\alpha = 0°$ and three torsional modes appear when $\alpha = 90°$ in the first eight modes, and the corresponding frequency parameters are larger for the case of $\alpha = 0°$ than for the case of $\alpha = 90°$. It means that the torsional stiffness around x-axis is smaller for the case of $\alpha = 90°$

Table 9
λ of E/E panels ($\Omega_1 = \Omega_2 = 30°$, $[\alpha/-\alpha/\alpha]$)

$\bar{k}$	α	1	2	3	4	5	6	7	8	9	10
0°	0°	2.521	3.624	12.03	12.79	24.01	27.02	35.89	47.44	56.22	63.34
	15°	2.472	3.770	12.22	12.73	24.20	27.17	36.19	47.31	56.13	64.14
	30°	2.380	3.988	12.19	12.76	24.35	27.27	36.38	46.71	55.44	65.27
	45°	2.307	3.993	11.74	12.75	24.22	26.82	35.78	45.50	53.81	65.69
	60°	2.299	3.759	11.33	12.45	24.11	25.97	34.92	43.65	51.61	65.76
	75°	2.359	3.451	10.93	12.20	23.72	25.52	34.47	41.67	49.63	64.87
	90°	2.406	3.298	10.72	12.11	23.37	25.46	34.38	40.74	48.79	64.17
15°	0°	2.203	4.325	11.15	13.88	24.28	26.90	36.62	47.78	55.95	63.30
	15°	2.080	4.352	10.67	13.86	24.09	25.96	36.46	46.35	54.94	63.63
	30°	2.011	4.394	10.45	13.72	23.91	25.60	36.27	45.06	53.99	64.09
	45°	1.999	4.278	10.41	13.27	23.79	25.13	35.53	43.90	52.48	64.19
	60°	1.998	4.117	10.31	12.90	24.05	24.34	34.89	42.43	50.71	64.64
	75°	1.946	4.123	9.967	13.01	23.15	25.13	34.87	40.82	49.44	64.53
	90°	1.865	4.357	9.664	13.52	22.76	26.06	35.39	40.16	49.46	64.24
30°	0°	1.760	5.933	9.922	16.29	24.43	28.43	38.90	48.66	56.42	62.67
	15°	1.613	5.776	9.328	15.73	23.73	26.82	38.40	45.75	55.12	62.71
	30°	1.514	5.709	8.851	15.50	22.91	26.29	38.05	43.49	54.35	62.58
	45°	1.475	5.593	8.701	15.17	22.53	25.90	37.38	42.01	53.27	62.45
	60°	1.448	5.507	8.757	14.85	22.63	25.63	36.95	40.74	52.03	63.52
	75°	1.404	5.563	8.818	14.83	22.69	26.17	37.13	39.73	51.33	64.50
	90°	1.373	5.778	8.888	15.25	22.91	27.41	37.54	40.16	51.92	64.62
45°	0°	1.447	6.744	10.36	18.68	25.96	33.94	42.29	51.80	59.15	62.72
	15°	1.299	6.195	10.09	17.16	25.48	31.64	41.78	48.70	58.72	61.98
	30°	1.184	5.776	9.771	16.09	24.88	30.08	41.15	46.58	58.82	61.20
	45°	1.131	5.522	9.662	15.46	24.48	29.06	40.06	45.12	58.51	60.70
	60°	1.109	5.362	9.930	15.02	24.93	28.30	39.45	43.99	57.22	62.54
	75°	1.088	5.260	10.42	14.73	25.98	27.91	39.49	43.55	56.41	64.95
	90°	1.085	5.286	10.89	14.84	26.99	28.50	39.86	44.65	56.93	65.98
60°	0°	1.276	5.812	13.53	18.10	33.08	37.08	50.91	56.80	61.16	70.87
	15°	1.142	5.255	13.26	16.47	32.47	34.60	50.88	55.10	60.70	70.28
	30°	1.020	4.743	12.89	14.98	31.22	32.47	50.04	53.52	60.34	70.31
	45°	0.955	4.437	12.61	14.22	29.93	31.13	47.90	52.14	60.44	68.84
	60°	0.932	4.301	12.58	14.14	29.03	31.07	46.18	50.93	62.16	67.18
	75°	0.921	4.236	12.65	14.44	28.40	31.98	45.41	50.11	63.51	67.49
	90°	0.925	4.261	12.85	14.85	28.53	33.07	45.31	50.83	64.23	68.59

than for the case of $\alpha = 0°$. In the cases of the twisting angle $\bar{k} = 30°$ and 60°, it is not obvious that modes change their orders in the first eight modes when the fiber orientation changes.

Figs. 8–10 show the changes in the modes of four-layer $[\alpha/-\alpha/\alpha/-\alpha]$ graphite/epoxy laminated panels when the fiber orientation changes. The vibration modes are similar to those of three-layer ones in shape, and the orders in the first eight modes are not necessarily the same. It can be seen that some modes change their orders with the change of the fiber orientation.

For three-layer $[\alpha/-\alpha/\alpha]$ E-glass/epoxy laminated panels shown in Figs. 5–7, it does not happen that lower vibration modes change their orders when the fiber angle changes from 0° to 90°, but the fifth and sixth modes in the case of $\alpha = 0°$ change to sixth and fifth ones in the case of $\alpha = 90°$.

Table 10
λ of E/E panels ($\Omega_1 = \Omega_2 = 60°$, $[\alpha/-\alpha/\alpha]$)

$\bar{k}$	α	1	2	3	4	5	6	7	8	9	10
0°	0°	2.997	3.636	12.20	14.72	26.48	30.27	45.71	53.27	71.41	75.16
	15°	2.945	3.779	12.47	14.62	26.87	30.50	46.06	53.44	72.40	75.47
	30°	2.868	3.971	12.92	14.29	27.51	30.69	46.23	53.43	73.59	75.20
	45°	2.825	3.966	12.74	14.23	27.76	30.34	45.24	52.95	71.94	75.09
	60°	2.852	3.769	12.03	14.53	27.90	29.61	43.57	52.05	69.05	75.74
	75°	2.951	3.497	11.42	14.74	27.86	29.16	42.18	50.78	66.49	76.92
	90°	3.048	3.324	11.17	14.80	27.65	29.15	41.62	50.11	65.36	77.41
15°	0°	2.886	3.813	12.22	14.69	26.32	30.36	44.93	53.80	70.81	74.79
	15°	2.775	3.916	12.21	14.54	26.39	30.11	44.91	53.27	70.64	75.00
	30°	2.730	4.001	12.49	14.17	26.77	30.03	44.78	52.83	71.02	74.77
	45°	2.760	3.889	12.43	13.93	26.86	29.72	43.65	52.34	69.67	74.21
	60°	2.837	3.670	11.86	14.17	26.96	29.26	42.17	51.67	67.23	74.80
	75°	2.832	3.593	11.32	14.53	27.16	29.09	41.29	50.68	65.27	76.35
	90°	2.710	3.770	11.15	14.82	27.47	29.26	41.42	50.23	64.86	77.52
30°	0°	2.629	4.316	12.37	14.59	26.04	30.57	43.29	54.80	69.17	73.93
	15°	2.495	4.346	12.00	14.48	25.83	29.81	42.95	53.67	67.95	74.01
	30°	2.451	4.364	12.05	14.17	26.04	29.42	42.72	52.74	67.71	73.84
	45°	2.472	4.251	12.07	13.83	26.05	29.13	41.71	52.06	66.51	73.26
	60°	2.480	4.150	11.69	13.95	26.17	28.88	40.61	51.44	64.62	74.00
	75°	2.406	4.245	11.22	14.41	26.51	29.00	40.31	50.60	63.34	76.01
	90°	2.312	4.520	11.08	14.92	27.18	29.45	41.12	50.34	63.72	77.79
45°	0°	2.296	5.184	12.39	14.94	26.21	30.82	42.14	55.66	66.87	73.14
	15°	2.153	5.124	11.72	14.77	25.78	29.50	41.53	54.06	64.89	73.04
	30°	2.091	5.104	11.47	14.61	25.83	28.79	41.27	52.66	64.31	72.86
	45°	2.085	5.018	11.44	14.30	25.83	28.44	40.50	51.67	63.36	72.35
	60°	2.061	4.993	11.34	14.22	25.96	28.36	39.84	50.90	62.11	73.42
	75°	1.995	5.152	11.07	14.59	26.28	28.84	40.10	50.08	61.63	75.97
	90°	1.942	5.462	10.97	15.23	27.12	29.65	41.48	49.94	62.84	78.26
60°	0°	1.950	6.255	11.89	16.70	27.30	31.44	43.00	56.25	64.84	72.74
	15°	1.803	6.055	11.32	16.06	26.84	29.58	42.29	54.02	63.08	72.44
	30°	1.728	5.970	10.92	15.80	26.72	28.54	42.04	52.06	62.70	72.15
	45°	1.707	5.868	10.88	15.48	26.70	28.00	41.46	50.61	62.17	71.72
	60°	1.683	5.809	11.05	15.18	26.77	28.07	41.10	49.56	61.54	73.29
	75°	1.638	5.869	11.22	15.20	26.89	29.00	41.64	48.80	61.66	76.45
	90°	1.617	6.063	11.39	15.69	27.80	30.13	43.32	48.85	63.47	79.00

4. Conclusions

The numerical method presented in this paper is a practical and effective method for analyzing the free vibrations of laminated cylindrical thin panels with twists and curvatures. Comparing the results obtained by the present method with the previous numerical and experimental results, it is found that the method can give accurate results when 12 integrating points are taken in the Gauss–Legendre integration and the polynomials having the proper number of the terms are adopted as displacement functions.

The effects of twist, curvature, material, the number of layers, fiber orientation and stacking sequence on the vibration frequency parameters and the mode shapes of laminated cylindrical thin panels are studied. It is known that the first frequency parameter decreases monotonically with increasing twisting angles, and the effect of increasing the fiber orientation angle on the first frequency parameter becomes large with an

Table 11
λ of E/E panels ($\Omega_1 = \Omega_2 = 90°$, $[\alpha/-\alpha/\alpha]$)

$\bar{k}$	α	1	2	3	4	5	6	7	8	9	10
0°	0°	3.597	3.609	13.15	16.15	28.30	34.95	54.42	58.92	80.23	93.71
	15°	3.513	3.772	13.42	16.07	28.82	35.13	54.78	59.36	81.52	93.73
	30°	3.453	3.920	13.86	15.82	29.71	35.18	54.91	59.96	83.36	92.33
	45°	3.399	3.921	13.70	15.83	30.10	34.73	53.72	60.27	83.27	89.48
	60°	3.364	3.824	13.01	16.24	30.27	33.88	51.71	60.50	82.53	86.51
	75°	3.333	3.732	12.41	16.57	30.61	32.94	50.04	60.10	82.59	84.24
	90°	3.310	3.699	12.17	16.67	30.86	32.43	49.35	59.67	82.16	83.90
15°	0°	3.411	3.816	13.02	16.32	28.07	34.95	52.94	59.91	79.96	93.04
	15°	3.318	3.926	13.18	16.14	28.33	34.89	53.09	59.76	80.45	92.77
	30°	3.320	3.966	13.50	15.83	28.98	34.76	53.07	59.84	81.73	91.18
	45°	3.378	3.834	13.31	15.78	29.18	34.27	51.78	60.01	81.34	88.38
	60°	3.473	3.620	12.70	16.15	29.32	33.62	49.95	60.40	80.39	85.95
	75°	3.316	3.707	12.21	16.52	29.84	33.00	48.71	60.30	80.33	84.69
	90°	3.158	3.890	12.12	16.72	30.63	32.66	48.63	60.16	80.98	84.55
30°	0°	3.180	4.140	12.86	16.59	27.52	35.01	50.31	61.04	78.96	91.50
	15°	3.071	4.203	12.85	16.37	27.54	34.69	50.17	60.50	78.67	90.81
	30°	3.077	4.201	13.11	16.00	28.01	34.40	50.12	60.07	79.35	89.16
	45°	3.133	4.065	12.99	15.83	28.12	33.94	48.96	59.94	78.73	86.66
	60°	3.138	3.965	12.47	16.09	28.27	33.53	47.38	60.40	77.72	84.94
	75°	3.016	4.073	12.05	16.47	28.95	33.29	46.56	60.62	77.74	84.66
	90°	2.892	4.297	12.06	16.76	30.12	33.25	47.01	60.84	79.04	85.18
45°	0°	2.889	4.666	13.01	16.65	27.14	35.21	47.65	61.47	77.04	89.61
	15°	2.769	4.676	12.75	16.45	26.90	34.63	47.18	60.73	76.14	88.43
	30°	2.761	4.659	12.93	16.06	27.21	34.17	47.04	59.97	76.30	86.81
	45°	2.791	4.552	12.90	15.77	27.29	33.75	46.02	59.57	75.58	84.77
	60°	2.771	4.509	12.49	15.91	27.47	33.60	44.73	59.94	74.66	83.90
	75°	2.677	4.638	12.11	16.28	28.22	33.75	44.32	60.25	74.99	84.54
	90°	2.592	4.883	12.14	16.64	29.63	34.03	45.28	60.70	77.02	85.65
60°	0°	2.558	5.439	13.61	16.51	27.45	35.56	45.45	61.65	74.93	86.85
	15°	2.435	5.378	13.08	16.32	26.95	34.72	44.72	60.82	73.56	85.65
	30°	2.411	5.352	13.10	15.97	27.07	34.08	44.50	59.84	73.29	84.46
	45°	2.424	5.272	13.13	15.61	27.09	33.65	43.60	59.12	72.40	83.11
	60°	2.401	5.253	12.85	15.64	27.19	33.71	42.63	59.15	71.57	83.18
	75°	2.333	5.377	12.51	15.97	27.83	34.21	42.63	59.23	72.19	84.66
	90°	2.281	5.612	12.55	16.38	29.28	34.78	44.04	59.65	74.83	86.19

increase in the twisting angle, and this effect is greater for graphite/epoxy laminated panels than for E-glass/epoxy one.

For strongly orthotropic graphite/epoxy laminated panels, it can be seen that some lower modes change their orders in the first eight modes with increasing fiber orientation angles and come back to original orders when the fiber orientation angle changes from 60° to 90° in the case of $\bar{k} = 0°$, but that cannot be seen for moderately orthotropic E-glass/epoxy one. The vibration modes for a three-layer laminated panel and a four-layer one are almost the same in shape and not necessarily the same in order, but the frequency parameters of the former are less than those of the latter. The torsional stiffness when $\alpha = 90°$ is less than that when $\alpha = 0°$.

The present method also illustrates the ability to deal with models having large twist and curvature.

Table 12
λ of G/E panels ($\Omega_1 = \Omega_2 = 30°$, $[\alpha/-\alpha/\alpha/-\alpha]$)

$\bar{k}$	α	1	2	3	4	5	6	7	8	9	10
0°	0°	1.912	2.194	8.101	9.221	13.83	19.83	24.81	28.86	40.30	41.65
	15°	1.814	2.637	8.857	9.046	15.53	20.05	25.96	31.71	41.62	41.76
	30°	1.589	3.174	8.306	10.03	17.21	20.84	27.30	34.18	41.52	46.18
	45°	1.487	3.221	7.739	10.04	17.06	20.47	26.53	33.85	40.29	46.31
	60°	1.449	2.787	7.590	8.620	17.06	17.54	24.69	29.05	35.61	40.63
	75°	1.400	2.059	6.469	7.359	13.47	16.65	22.72	24.35	30.24	33.51
	90°	1.391	1.602	5.172	7.214	11.17	16.11	19.32	24.32	28.78	29.87
15°	0°	1.701	2.532	8.216	9.046	14.09	20.22	24.24	29.42	39.93	41.44
	15°	1.696	2.892	8.489	9.442	15.75	20.35	25.70	32.50	40.73	41.97
	30°	1.505	3.484	7.863	10.74	17.23	21.15	27.58	34.64	41.49	45.81
	45°	1.341	3.685	7.149	10.96	16.91	20.75	27.17	33.75	40.70	45.66
	60°	1.220	3.336	6.648	9.820	16.06	18.69	25.12	28.83	35.87	40.23
	75°	1.050	2.720	5.709	8.269	13.21	17.11	22.44	24.89	30.42	33.84
	90°	0.912	2.394	4.889	7.517	11.31	15.95	19.58	24.65	28.57	30.51
30°	0°	1.440	3.276	7.918	9.750	15.12	21.23	23.81	30.53	38.97	41.08
	15°	1.432	3.714	7.624	10.97	16.39	21.68	25.85	34.27	39.37	41.93
	30°	1.293	4.482	6.897	12.81	16.98	22.90	28.56	36.31	41.62	44.49
	45°	1.096	4.779	6.159	12.98	16.31	22.34	28.45	34.27	42.22	43.89
	60°	0.928	4.139	5.904	11.12	15.56	20.31	25.23	29.77	36.60	40.81
	75°	0.745	3.296	5.440	8.766	13.79	17.27	22.81	26.22	31.34	34.88
	90°	0.629	2.814	5.141	7.434	12.54	15.14	21.01	25.48	29.10	31.51
45°	0°	1.256	4.347	7.211	12.90	16.51	23.59	25.68	31.28	39.06	41.42
	15°°	1.210	4.839	6.897	14.23	16.93	26.19	27.29	35.04	40.22	43.02
	30°	1.085	5.311	6.633	14.73	17.78	26.74	30.44	39.77	40.83	45.68
	45°	0.903	4.549	7.032	13.05	18.02	24.75	29.51	37.79	41.69	45.82
	60°	0.736	3.626	7.051	10.47	17.76	21.03	25.63	33.06	37.66	43.17
	75°	0.575	2.806	6.671	8.046	16.00	16.95	24.47	28.26	33.23	36.28
	90°	0.487	2.379	6.372	6.911	13.77	15.58	23.37	26.51	31.15	32.85
60°	0°	1.157	4.855	7.772	15.55	19.96	27.72	30.16	32.93	40.35	44.49
	15°	1.088	4.798	8.073	14.93	21.91	28.55	32.94	37.41	42.11	48.81
	30°	0.950	4.416	8.772	13.55	22.92	27.77	35.30	40.74	44.58	52.53
	45°	0.777	3.635	9.191	11.47	21.65	25.03	33.37	40.31	43.51	50.92
	60°	0.617	2.851	8.681	9.454	19.95	21.62	27.62	36.99	40.09	45.78
	75°	0.478	2.201	6.855	8.661	15.64	20.21	25.85	30.87	35.96	38.33
	90°	0.409	1.888	5.843	8.409	13.27	18.82	25.56	27.92	34.27	35.18

Appendix A

The variables in Eq. (1) and other equations in this paper are defined as

$$A = 1 - \frac{r}{R}\sin(kx + \phi - \theta) + \frac{e}{R}\sin(kx + \phi), \qquad B = \sqrt{e^2k^2\sin^2\theta + A^2},$$

$$p = -r\cos(kx + \phi - \theta) + e\cos(kx + \phi), \qquad q = \frac{Ar}{R}\cos(kx + \phi - \theta) + e^2k^2\sin\theta\cos\theta,$$

$$h_1 = A - \frac{e}{R}\sin\theta\cos(kx + \phi - \theta), \qquad h_2 = \frac{A}{R}\cos(kx + \phi - \theta) + ek^2\sin\theta,$$

Table 13
λ of G/E panels ($\Omega_1 = \Omega_2 = 60°$, $[\alpha/-\alpha/\alpha/-\alpha]$)

$\bar{k}$	α	1	2	3	4	5	6	7	8	9	10
0°	0°	2.196	2.218	7.962	10.27	15.69	21.21	31.47	31.81	45.77	50.84
	15°	2.099	2.622	8.825	10.05	17.44	21.74	33.04	34.69	48.72	53.49
	30°	1.868	3.120	9.560	9.973	19.72	22.61	34.63	37.84	54.44	54.67
	45°	1.854	3.104	9.433	9.982	20.04	22.65	33.28	38.60	52.44	54.73
	60°	1.957	2.658	8.707	9.616	20.11	20.35	29.72	35.89	45.73	52.34
	75°	1.997	2.012	6.777	9.548	16.60	20.55	27.18	29.98	37.91	46.79
	90°	1.620	2.034	5.649	9.499	14.52	20.51	26.59	27.20	34.26	42.61
15°	0°	2.077	2.345	7.930	10.20	15.44	21.28	29.99	32.55	45.47	50.63
	15°	2.072	2.664	8.796	10.03	17.24	21.74	31.91	35.24	48.44	52.95
	30°	1.863	3.167	9.533	10.05	19.56	22.68	34.03	38.07	54.10	54.34
	45°	1.815	3.219	9.271	10.23	19.99	22.70	33.09	38.65	52.31	54.51
	60°	1.822	2.876	8.571	9.803	20.19	20.31	29.76	35.78	45.66	52.39
	75°	1.640	2.455	6.743	9.602	16.49	20.64	27.27	29.88	37.90	46.79
	90°	1.410	2.336	5.638	9.469	14.44	20.45	26.13	27.61	34.23	42.46
30°	0°	1.916	2.567	8.002	9.939	14.87	21.48	27.91	32.70	44.52	50.09
	15°	1.967	2.852	8.956	9.819	16.80	21.92	30.05	35.68	47.74	51.78
	30°	1.817	3.383	9.324	10.47	19.24	22.97	32.93	38.51	53.37	53.49
	45°	1.697	3.590	8.891	10.88	19.93	22.88	32.79	38.75	52.10	53.84
	60°	1.582	3.378	8.224	10.27	19.98	20.59	29.94	35.35	45.62	52.50
	75°	1.341	3.003	6.664	9.675	16.29	20.69	27.49	29.54	37.95	46.71
	90°	1.148	2.833	5.656	9.326	14.31	20.18	25.49	28.20	34.23	42.22
45°	0°	1.715	2.976	8.625	9.407	14.58	21.93	25.86	32.51	43.18	49.06
	15°	1.767	3.303	9.259	9.756	16.55	22.38	28.31	35.94	46.55	50.39
	30°	1.679	3.925	8.792	11.54	19.00	23.53	32.08	39.02	51.88	52.81
	45°	1.520	4.242	8.340	11.93	19.97	23.20	32.85	38.78	52.07	52.60
	60°	1.345	4.004	7.810	10.93	19.62	21.15	30.48	34.50	45.81	52.76
	75°	1.101	3.514	6.688	9.693	16.24	20.59	27.83	29.20	38.32	46.85
	90°	0.938	3.211	5.949	8.953	14.45	19.53	25.18	28.82	34.59	42.22
60°	0°	1.499	3.611	8.647	10.37	15.23	22.89	24.71	32.80	42.04	47.25
	15°	1.527	4.039	8.455	11.63	17.00	23.40	27.74	36.61	45.01	49.16
	30°	1.476	4.780	8.091	13.38	19.16	24.57	32.36	39.96	49.37	52.81
	45°	1.323	4.921	7.953	13.23	20.22	23.90	33.70	38.71	50.68	52.75
	60°	1.137	4.350	7.842	11.51	19.51	21.92	31.24	33.72	46.68	53.15
	75°	0.912	3.595	7.293	9.472	16.66	20.23	28.08	29.57	39.46	47.36
	90°	0.779	3.147	6.917	8.315	15.06	18.52	25.61	29.43	35.71	42.59

$$h_3 = A\cos\theta - \frac{r}{R}\sin\theta\cos(kx+\phi-\theta), \qquad h_4 = \frac{ek^2}{B^2R}p\sin\theta - \frac{1}{R}\sin(kx+\phi-\theta),$$

$$p_1 = \frac{1}{B}\left\{\frac{A}{r} + h_4 - \frac{ek^2}{B^2r}h_3(r-e\cos\theta)\right\}, \qquad F = B(1+zp_1).$$

Appendix B

The nonzero elements of matrix $\boldsymbol{G}$ are

$$G_{1,1} = B, \qquad G_{1,2} = \frac{Bk}{r}(r-e\cos\theta), \qquad G_{1,3} = \frac{Ak}{BR}p, \qquad G_{1,6} = \frac{1}{Br}q,$$

Table 14
λ of G/E panels ($\Omega_1 = \Omega_2 = 90°$, $[\alpha/-\alpha/\alpha/-\alpha]$)

$\bar{k}$	α	1	2	3	4	5	6	7	8	9	10
0°	0°	2.199	2.613	8.520	10.88	17.22	23.87	34.06	37.44	53.12	58.78
	15°	2.488	2.593	9.395	10.81	18.99	24.47	37.56	38.95	56.61	63.75
	30°	2.234	3.056	10.52	10.58	21.58	25.16	40.62	41.81	62.73	65.51
	45°	2.246	3.017	10.54	10.63	22.15	25.26	39.30	43.16	62.53	63.14
	60°	2.396	2.576	9.285	10.90	22.05	23.27	34.76	42.16	55.83	59.12
	75°	1.981	2.465	7.412	10.83	19.73	22.67	30.40	36.79	46.54	57.13
	90°	1.633	2.518	6.355	10.76	17.79	23.33	28.97	33.38	41.98	53.79
15°	0°	2.184	2.616	8.373	10.93	16.89	23.82	33.33	37.12	52.94	58.59
	15°	2.437	2.640	9.224	10.94	18.71	24.31	36.54	38.99	56.48	63.06
	30°	2.234	3.074	10.39	10.74	21.34	25.12	39.68	42.04	62.18	65.18
	45°	2.225	3.076	10.52	10.74	22.02	25.30	38.86	43.15	62.04	63.17
	60°	2.245	2.764	9.291	10.95	22.02	23.32	34.55	42.11	55.82	59.06
	75°	1.891	2.589	7.405	10.84	19.60	22.83	30.32	36.73	46.53	56.92
	90°	1.582	2.601	6.341	10.72	17.70	23.30	28.88	33.33	41.95	53.25
30°	0°	2.129	2.664	8.122	10.97	16.06	23.61	31.62	36.21	51.57	58.60
	15°	2.316	2.779	9.033	11.07	18.04	24.08	34.72	38.55	55.68	62.03
	30°	2.209	3.180	10.46	10.86	20.84	25.15	38.22	41.96	60.56	64.88
	45°	2.146	3.286	10.48	11.03	21.78	25.43	37.97	43.04	60.94	63.23
	60°	2.038	3.093	9.312	11.03	21.96	23.42	34.00	41.83	55.85	58.84
	75°	1.715	2.874	7.413	10.80	19.33	23.08	30.01	36.40	46.53	56.21
	90°	1.460	2.824	6.330	10.58	17.45	23.21	28.62	33.16	41.89	52.11
45°	0°	2.002	2.871	8.149	10.92	15.26	23.26	29.79	35.15	49.13	58.96
	15°	2.130	3.069	9.159	11.04	17.41	23.88	32.77	37.83	53.52	61.57
	30°	2.104	3.487	10.66	11.00	20.41	25.26	36.67	41.56	58.32	64.49
	45°	2.000	3.686	10.41	11.45	21.70	25.50	36.89	42.79	59.51	62.96
	60°	1.824	3.529	9.344	11.13	21.92	23.52	33.35	41.17	55.71	58.55
	75°	1.524	3.251	7.485	10.67	18.96	23.28	29.68	35.72	46.46	55.35
	90°	1.312	3.130	6.411	10.31	17.11	22.94	28.27	32.89	41.78	50.91
60°	0°	1.807	3.302	8.726	10.79	15.24	23.06	28.46	34.74	46.98	59.07
	15°	1.900	3.565	9.789	10.87	17.45	23.91	31.12	37.73	51.29	60.68
	30°	1.922	4.052	10.61	11.63	20.52	25.48	35.29	41.42	56.45	63.43
	45°	1.811	4.263	10.36	11.94	22.07	25.40	35.85	42.60	57.94	62.09
	60°	1.612	4.034	9.459	11.23	21.86	23.60	32.81	40.11	55.03	58.38
	75°	1.338	3.640	7.738	10.48	18.56	23.24	29.53	34.81	46.11	54.60
	90°	1.165	3.413	6.752	9.924	16.78	22.42	27.88	32.69	41.57	49.89

$$G_{1,12} = h_4 - \frac{ek^2}{B^2 r} h_3 (r - e\cos\theta), \qquad G_{2,1} = \frac{A}{r} + h_4, \qquad G_{2,2} = \frac{k}{r}\{h_1 + h_4(r - e\cos\theta)\},$$

$$G_{2,3} = \frac{k}{R}\left[\frac{ek^2}{B^2 r} p\cos\theta(r - e\cos\theta) - \frac{2Aek^2}{B^4 R} p^2 \sin\theta - \frac{2ek^2}{B^4 r} pq \sin\theta(r - e\cos\theta)\right.$$
$$\left. - \frac{e^2k^2}{B^2}\sin^2\theta\cos(kx + \phi - \theta) + \frac{A^2}{B^2 r} p - \cos(kx + \phi - \theta)\right],$$

$$G_{2,4} = -\frac{ek}{B^2 r} h_3, \qquad G_{2,5} = \frac{ek^2}{B^2 r^2} h_3 (e\cos\theta - r),$$

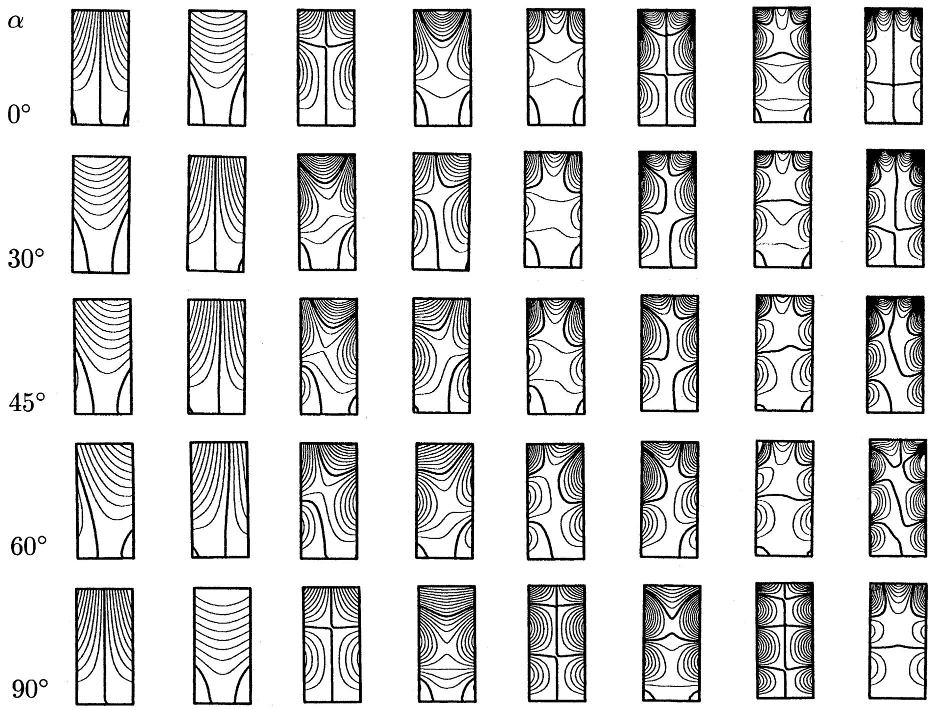

Fig. 2. Mode shapes of G/E panels ($\bar{k} = 0°$, $[\alpha/-\alpha/\alpha]$).

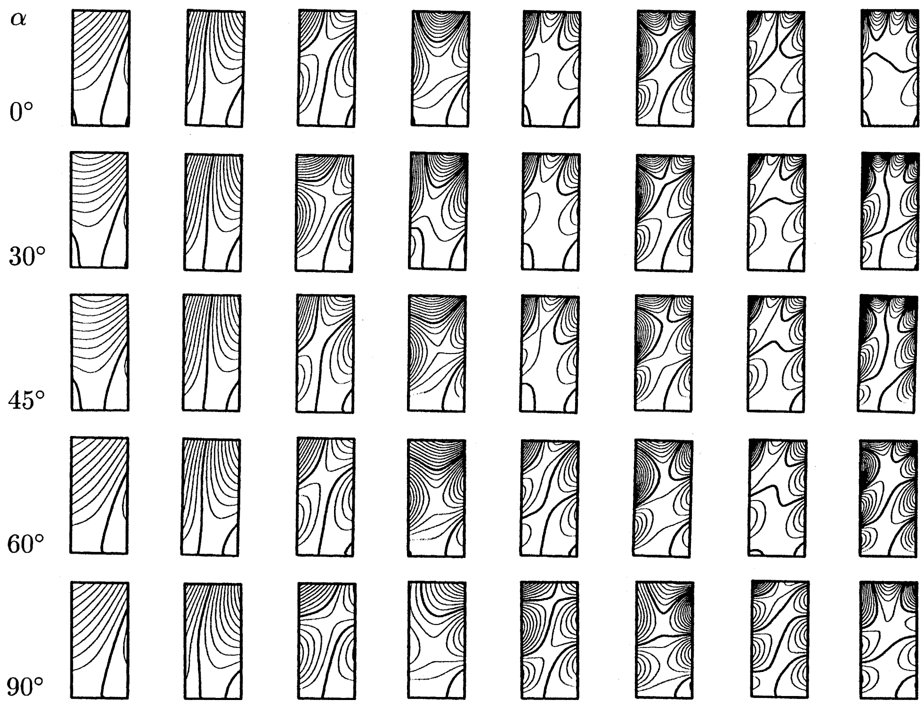

Fig. 3. Mode shapes of G/E panels ($\bar{k} = 30°$, $[\alpha/-\alpha/\alpha]$).

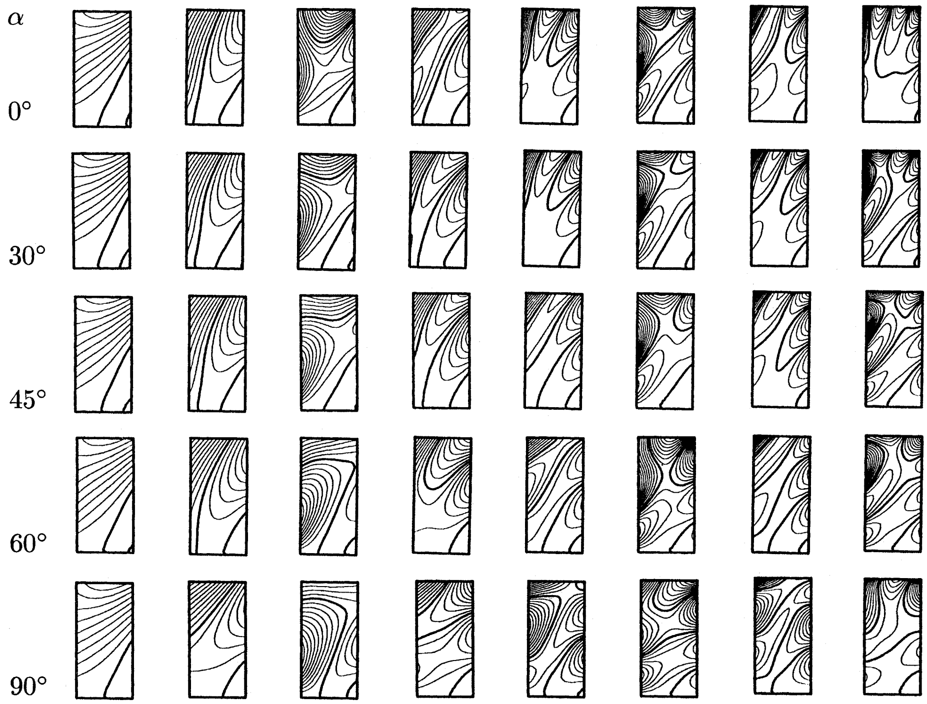

Fig. 4. Mode shapes of G/E panels ($\bar{k} = 60°$, $[\alpha/-\alpha/\alpha]$).

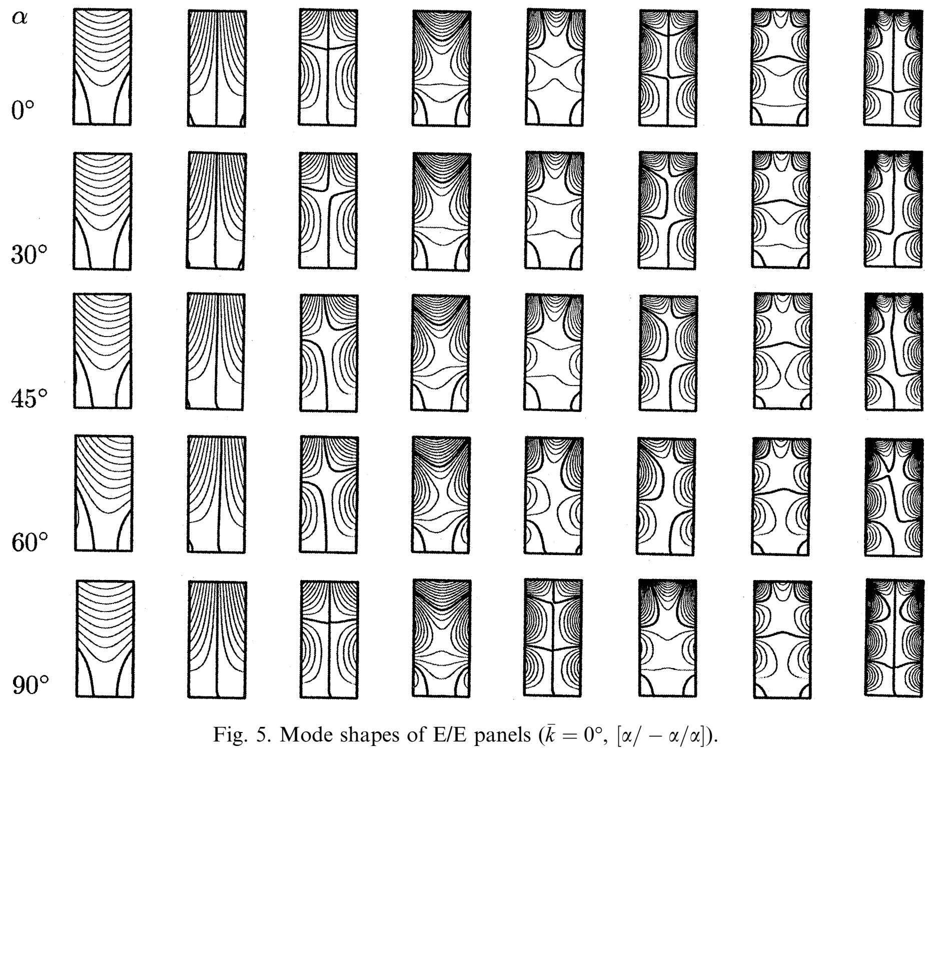

Fig. 5. Mode shapes of E/E panels ($\bar{k} = 0°$, $[\alpha/-\alpha/\alpha]$).

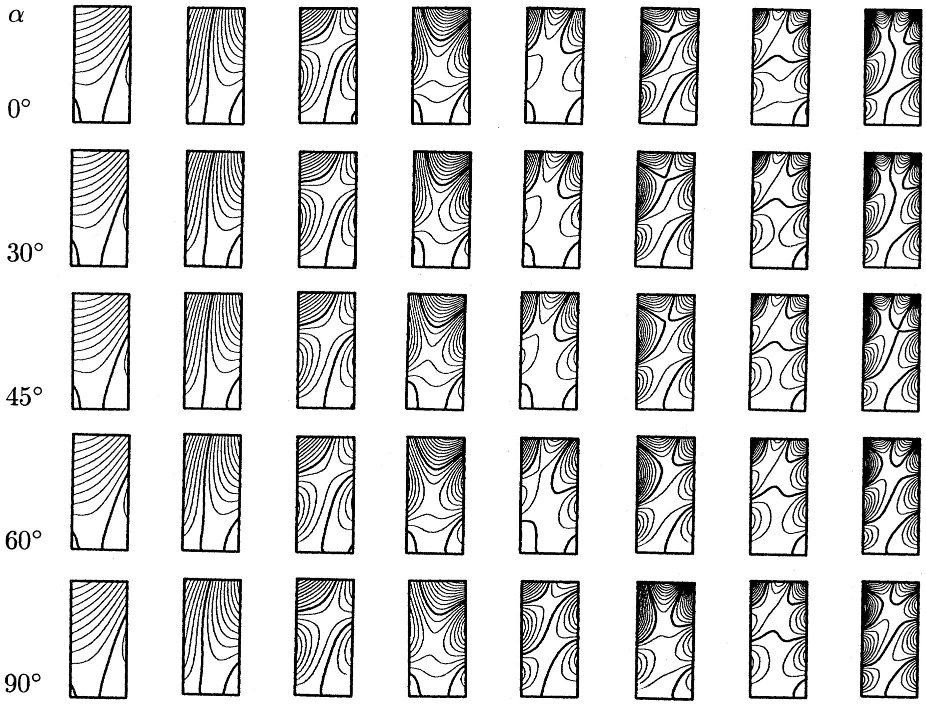

Fig. 6. Mode shapes of E/E panels ($\bar{k} = 30°$, $[\alpha/-\alpha/\alpha]$).

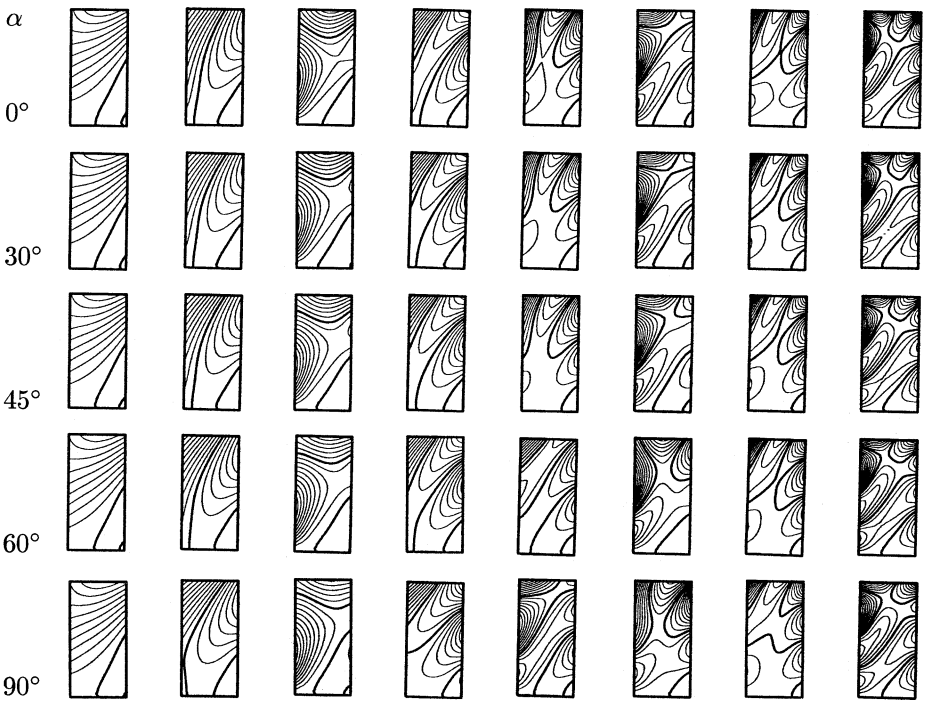

Fig. 7. Mode shapes of E/E panels ($\bar{k} = 60°$, $[\alpha/-\alpha/\alpha]$).

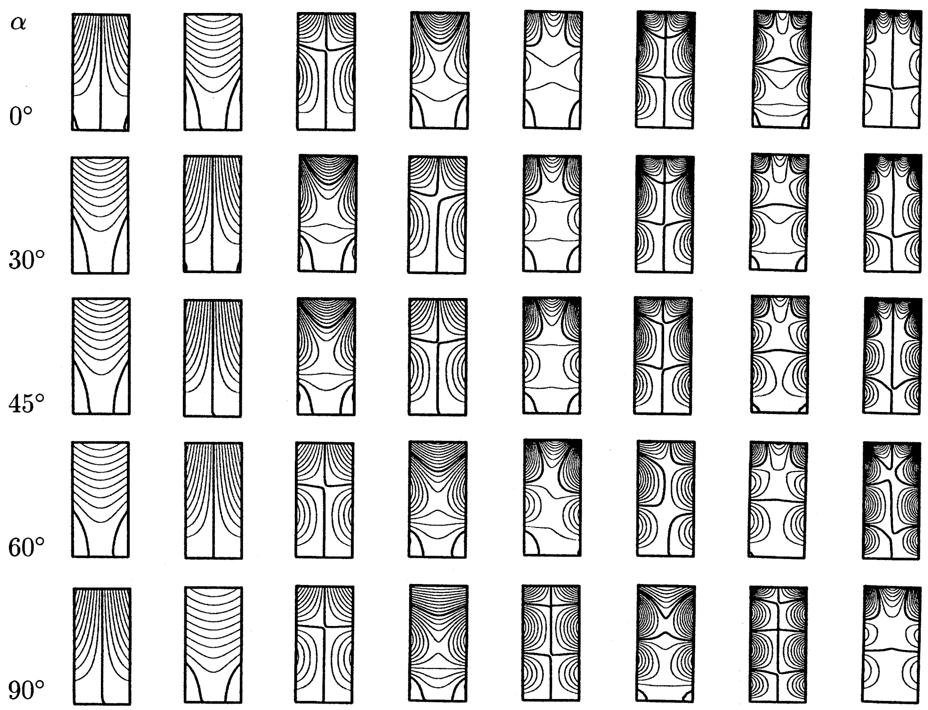

Fig. 8. Mode shapes of G/E panels ($\bar{k} = 0°$, $[\alpha/-\alpha/\alpha/-\alpha]$).

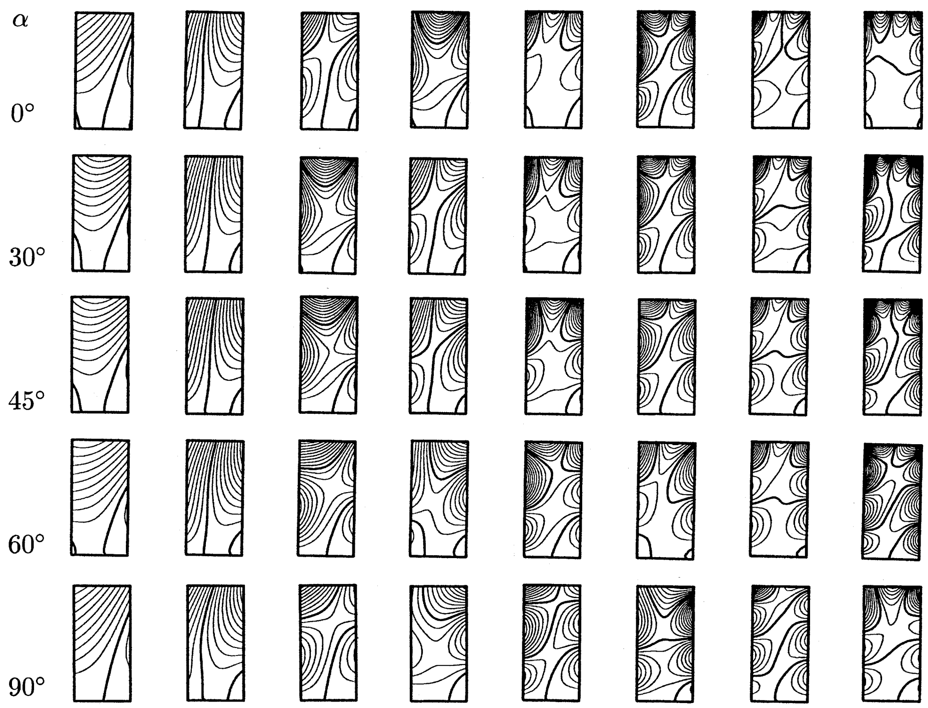

Fig. 9. Mode shapes of G/E panels ($\bar{k} = 30°$, $[\alpha/-\alpha/\alpha/-\alpha]$).

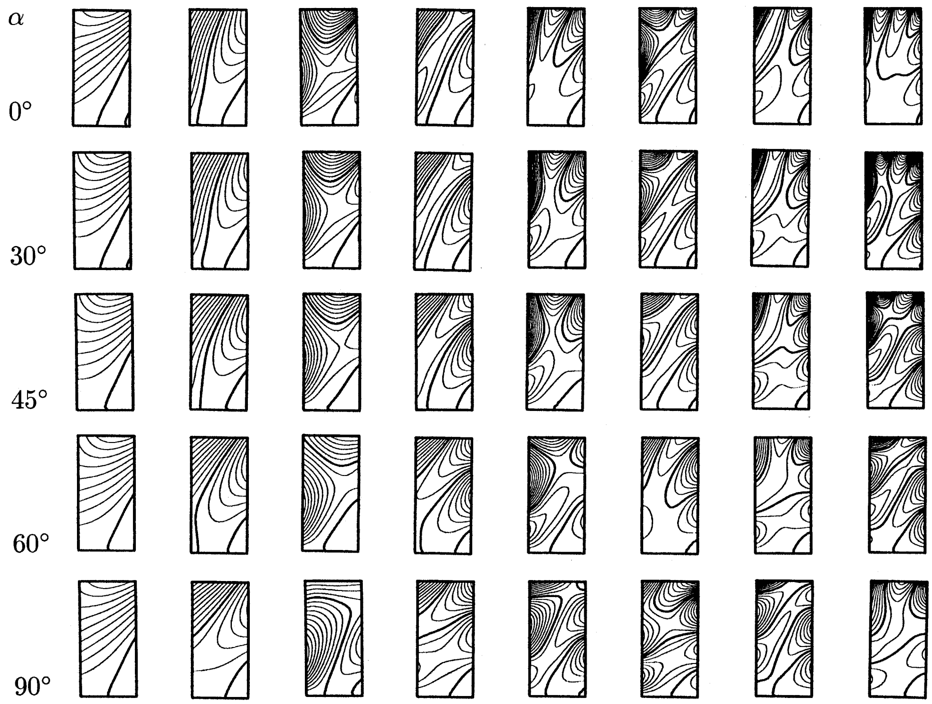

Fig. 10. Mode shapes of G/E panels ($\bar{k} = 60°$, $[\alpha/-\alpha/\alpha/-\alpha]$).

$$G_{2,6} = \frac{1}{r}\left[\frac{ek^2}{B^2R}(r - e\cos\theta)\cos\theta\cos(kx+\phi-\theta) + \frac{2Aek^2}{B^4R}ph_3 + \frac{2ek^2}{B^4r}h_3q(r-e\cos\theta) + \frac{1}{R}\cos(kx+\phi-\theta) + \frac{A}{B^2}h_2\right],$$

$$G_{2,7} = -\frac{1}{B}, \qquad G_{2,8} = -\frac{k^2}{Br^2}(e\cos\theta - r)^2, \qquad G_{2,9} = \frac{2k}{Br}(e\cos\theta - r),$$

$$G_{2,10} = \frac{k}{B^3}\left[\frac{A}{R}p + \frac{1}{r}q(r - e\cos\theta)\right],$$

$$G_{2,11} = -\frac{1}{Br}\left\{k^2(r-e\cos\theta)\left(\frac{e}{r}\sin\theta - \frac{A}{B^2R}p\right) + \frac{1}{B^2r}q\left[B^2 - k^2(e\cos\theta - r)^2\right]\right\},$$

$$G_{2,12} = \frac{1}{Br}\left(Ah_4 - \frac{ek^2}{B^2}h_1h_3\right), \qquad G_{3,4} = -\frac{Aek}{B^3r^2}h_3, \qquad G_{3,5} = -\frac{ek^2}{B^3r^2}h_1h_3,$$

$$G_{3,7} = -\frac{A}{B^2r}, \qquad G_{3,8} = \frac{k^2}{B^2r^2}h_1(e\cos\theta - r), \qquad G_{3,9} = \frac{k}{B^2r^2}[A(e\cos\theta - r) - rh_1],$$

$$G_{3,10} = \frac{k}{B^4 r}\left(\frac{A^2}{R}p + h_1 q\right),$$

$$G_{3,11} = -\frac{1}{r^2}\left[\frac{A^2k^2}{B^4R}p(e\cos\theta - r) + \frac{1}{R}\cos(kx+\phi-\theta) + \frac{k^2}{B^4}h_1 q(e\cos\theta - r) + \frac{ek^2}{B^2}h_1\sin\theta\right],$$

$$G_{4,2} = \frac{Bk}{r}(e\cos\theta - r),$$

$$G_{4,5} = \frac{B}{r}, \qquad G_{4,12} = \frac{A}{r}, \qquad G_{5,1} = \frac{ek^2}{B^2 r}h_3(e\cos\theta - r),$$

$$G_{5,2} = \frac{k}{r}[h_4(e\cos\theta - r) - h_1], \qquad G_{5,3} = \frac{e^2k^3}{B^2Rr}p\sin^2\theta, \qquad G_{5,4} = \frac{ek}{B^2 r}h_3,$$

$$G_{5,5} = \frac{1}{r}\left(h_4 + \frac{A}{r}\right), \qquad G_{5,6} = -\frac{2e^2k^2}{B^2r^2}h_3\sin\theta, \qquad G_{5,8} = -\frac{B}{r^2}, \qquad G_{5,10} = -\frac{ek}{Br}\sin\theta,$$

$$G_{5,11} = \frac{ek^2}{Br^2}(e\cos\theta - r)\sin\theta, \qquad G_{5,12} = \frac{1}{Br}\left(Ah_4 - \frac{ek^2}{B^2}h_1h_3\right), \qquad G_{6,1} = -\frac{ek^2}{B^3 r}h_1h_3,$$

$$G_{6,3} = \frac{ek^3}{B^3Rr}\left[eph_4\sin^2\theta - h_3(e\cos\theta - r)\cos(kx+\phi-\theta) + \frac{A}{B^2}ph_1h_3\right],$$

$$G_{6,4} = \frac{Aek}{B^3r^2}h_3, \qquad G_{6,6} = \frac{e^2k^2}{B^3r^2}h_3\left[\frac{1}{R}\sin\theta\sin(kx+\phi-\theta) - h_4\sin\theta + \frac{1}{B^2}h_2h_3\right],$$

$$G_{6,8} = -\frac{1}{r^2}h_4, \qquad G_{6,9} = -\frac{ek}{B^2r^2}h_3, \qquad G_{6,10} = \frac{ek}{B^4 r}\left(h_2h_3 - B^2h_4\sin\theta\right),$$

$$G_{6,11} = \frac{ek^2}{B^4r^2}(e\cos\theta - r)\left(B^2h_4\sin\theta - h_2h_3\right), \qquad G_{7,1} = k(e\cos\theta - r),$$

$$G_{7,2} = \frac{1}{r}\left[B^2 - k^2(e\cos\theta - r)^2\right], \qquad G_{7,4} = 1, \qquad G_{7,5} = \frac{k}{r}(r - e\cos\theta), \qquad G_{7,6} = -\frac{ek}{r}\sin\theta,$$

$$G_{7,12} = -\frac{2ek}{Br}h_3, \qquad G_{8,1} = \frac{2Ak}{Br}(e\cos\theta - r), \qquad G_{8,2} = \frac{2}{Br}\left[B^2h_4 - k^2h_1(r - e\cos\theta)\right],$$

$$G_{8,3} = \frac{2ek^2}{BRr}\left[\frac{2A}{B^2}ph_3 + (r - e\cos\theta)\cos(kx+\phi)\right], \qquad G_{8,4} = \frac{2A}{Br}, \qquad G_{8,5} = \frac{2Ak}{Br^2}(r - e\cos\theta),$$

$$G_{8,6} = \frac{2ek}{Br}\left[\frac{1}{R}\sin\theta\sin(kx+\phi-\theta) + \frac{2}{B^2 r}h_3 q\right], \qquad G_{8,8} = \frac{2k}{r^2}(e\cos\theta - r), \qquad G_{8,9} = -\frac{2}{r},$$

$$G_{8,10} = \frac{2}{B^2 r}q, \qquad G_{8,11} = -\frac{2k}{B^2r^2}q(e\cos\theta - r),$$

$$G_{9,3} = \frac{k^2}{B^2}\left[\frac{e^2k^2}{B^2r}(1-A)h_3\sin\theta + \frac{1}{Rr}ph_1 + \frac{e}{R^2r}(r-e\cos\theta)\sin\theta\cos^2(kx+\phi-\theta) - \frac{2Ae^2k^2}{B^4R^2r}p^2h_3\sin\theta \right.$$
$$- \frac{e}{Rr}h_3\cos(kx+\phi-\theta) + \frac{e}{Rr}ph_4\cos\theta - \frac{e}{R}h_4\sin\theta\sin(kx+\phi-\theta) - \frac{2e}{B^2Rr}ph_4q\sin\theta$$
$$\left. + \frac{1}{Rr}h_1(r-e\cos\theta)\cos(kx+\phi-\theta)\right], \qquad G_{9,7} = -\frac{ek}{B^3r}h_3,$$

$$G_{9,8} = \frac{k}{Br^2}[h_4(e\cos\theta - r) - h_1], \qquad G_{9,9} = \frac{1}{Br}\left[\frac{ek^2}{B^2r}h_3(e\cos\theta - r) - \frac{A}{r} - h_4\right],$$

$$G_{9,10} = \frac{1}{Br}\left[\frac{1}{R}\cos(kx+\phi-\theta) + \frac{1}{B^2}h_4q + \frac{Aek^2}{B^4R}ph_3\right],$$

$$G_{9,11} = -\frac{k}{Br}\left[\frac{1}{Rr}(e\cos\theta - r)\cos(kx+\phi-\theta) + \frac{e}{B^2r}h_2h_3 + \frac{ek^2}{B^2Rr}p(e\cos\theta - r)\cos\theta \right.$$
$$\left. - \frac{1}{B^2Rr}q(e\cos\theta - r)\sin(kx+\phi-\theta)\right].$$

References

Hu, X.X., Tsuiji, T., 1999. Free vibration analysis of curved and twisted cylindrical thin panels. Journal of Sound and Vibration 219, 63–88.

Leissa, A.W., 1973. Vibration of shells, NASA SP-288. US Government Printing Office, Washington DC, US.

Leissa, A.W., 1981a. Vibrational aspects of rotating turbomachineery blades. Applied Mechanics Reviews 34, 629–635.

Leissa, A.W., 1981b. Updata to vibrational aspects of rotating turbomachinery blades. Applied Mechanics Updata, ASME Press 359–362.

Leissa, A.W., Lee, J.K., Wang, A.J., 1982. Rotating blade vibration analysis using shells. Journal of Engineering Power 104, 296–302.

Leissa, A.W., Lee, J.K., Wang, A.J., 1983. Vibrations of cantilevered doubly-curved shallow shells. International Journal of Solids and Structures 19, 411–424.

Liew, K.M., Lim, C.M., Ong, L.S., 1994. Vibration of pretwisted cantilever shallow conical shells. International Journal of Solids and structures 31, 2463–2476.

Liew, K.M., Lim, M.K., Lim, C.W., 1995. Effects of initial twist and thickness variation on the vibration behavior of shallow conical shells. Journal of Sound and Vibration 180, 271–296.

Liew, K.M., Lim, C.W., 1996. Vibratory characteristics of pretwisted cantilever trapezoids of unsymmetric laminates. AIAA Journal 34, 1041–1050.

Liew, K.M., Lim, C.W., Kitipornchai, S., 1997. Vibration of shallow shells: A review with bibliography. Applied Mechanics Reviews 50, 431–444.

Lim, C.W., Liew, K.M., 1995. Vibration of pretwisted cantilever trapezoidal symmetric laminates. Acta Mechanica 111, 192–208.

Lim, C.W., Liew, K.M., Kitipornchai, S., 1997. Free vibration of pretwisted cantilevered composite shallow conical shells. AIAA Journal 35, 327–333.

Lim, C.W., Liew, K.M., Kitipornchai, S., 1998. Vibration of cantilevered laminated composite shallow conical shells. International Journal of Solids and Structures 35, 1695–1707.

Qatu, M.S., Leissa, A.W., 1991a. Natural frequencies for cantilevered doubly-curved laminated composite shallow shells. Composite Structures 17, 227–255.

Qatu, M.S., Leissa, A.W., 1991b. Vibration studies for laminated composite twisted cantilevered plates. International Journal of Mechanical Science 33, 927–940.

Tsuiji, T., Sueoka, T., 1990. Vibration analysis of twisted thin cylindrical panels by using the Rayleigh–Ritz method. Japan Society of Mechanical Engineers International Journal Series 3 33, 501–505.

Tsuiji, T., Syugyo, M., Yamashita, T., 1996. Free vibration analysis for composite laminated twisted cantilevered thin plates. Transactions of the Japan Society of Mechanical Engineers 62, 163–169.